Flow Near Hemispherical Depressions

Felix Kaplanski, Medhat Hussainov, Alexander Kartushinsky and Ülo Rudi

Department of Aeromechanics, Estonian Energy Research Institute
Paldiski mnt. 1, Tallinn, 10137, Estonia
aeromeh@online.ee

ABSTRACT

An experimental study of the influence of a special form of extended surfaces with hemispherical depressions on their aerodynamic drag is presented. By using the technique of aerodynamic weighing, it is shown that some of these, allowing us to enhance convective heat transfer, will not produce any significant rise in the drag. Preliminary computations aimed at increasing understanding of this phenomenon are provided.

1. INTRODUCTION

Drag reduction is a field of study in fluid mechanics in many engineering disciplines, such as in mechanical, chemical, civil, aeronautical, marine, and automotive engineering. It is also relevant to physics and architecture. The drag reduction phenomenon produced by riblets is closely connected to the heat and mass transfer in the vicinity of solid boundaries. At the same time, a tremendous number of work has been devoted to the drag reduction produced by riblets, but there is a lack of investigations dealing with the riblet effect on the heat transfer phenomenon. Therefore, investigations pertaining to an optimal surface with respect to the correlation between the drag reduction of a surface and the benefit of heat enhancement from it are at present unknown. However, this issue is very important from the practical point of view, for instance, in the designing of HX (heat exchangers).

The main goal of the study is investigation of the flow near some special form of extended surfaces with hemispherical depressions. Such a shape is shown in Fig.1. According to the hypothesis in /1/ this form of extended surface allows us to enhance convective heat transfer in comparison with a smooth surface without any significant increase in aerodynamic drag. There are experimental data confirming the enhancement of heat transfer in this case /2/. At the same time, the aerodynamic drag modification in this case was unexpected, which has encouraged us to focus on this phenomenon. We carried out experimental investigations of the influence of such a surface shape on the aerodynamic drag by the aerodynamic weighing technique and have provided preliminary computations aimed at increasing understanding of this phenomenon.

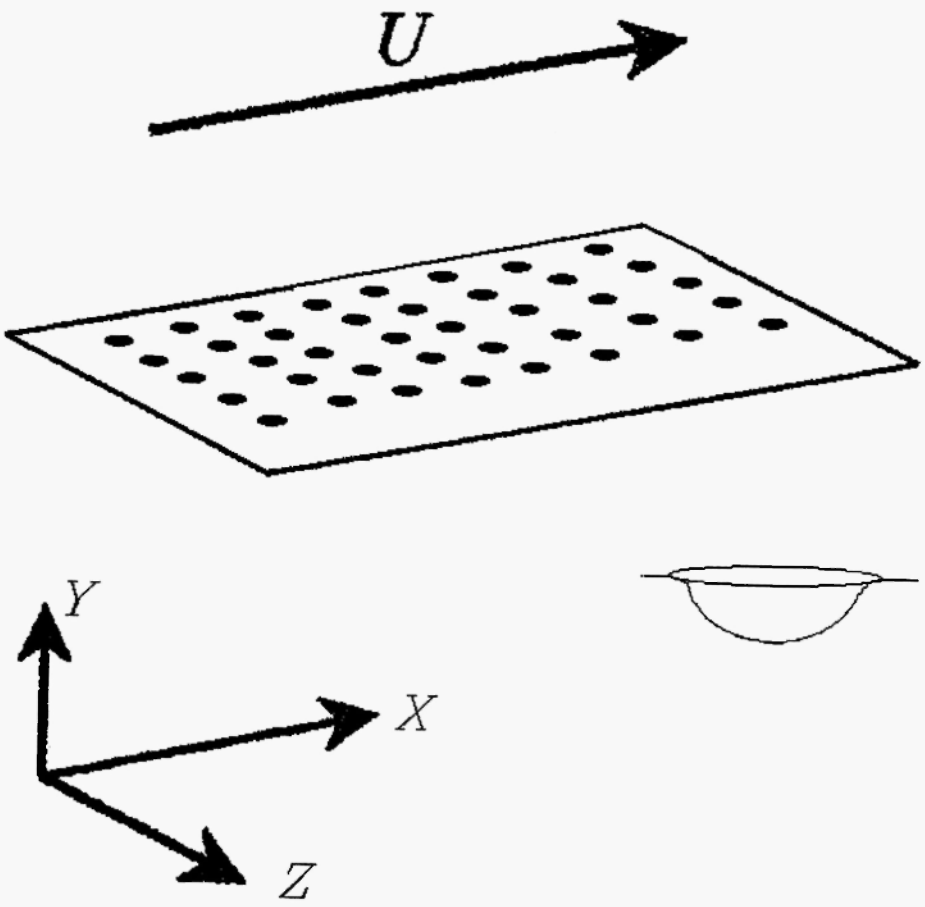

Fig. 1: The shape of extended surfaces.

2. EXPERIMENTAL RESULTS

The experiments were carried out in a disconnected vertical, two-phase wind-channel with an open working space (Fig. 2). The arrangement of the wind-channel allowed us to investigate both single- and two-phase flows. The diameter of the working space of the wind-channel was 150 mm. In the given test series, we investigated a single-phase flow past the plates for laminar and turbulent regimes. The velocities of the main flow in the streamwise downstream direction U_∞ were 9.4 and 22 m/s, respectively. In the experiments we used a smooth flat plate and flat plates with hemispherical depressions on the bilateral sides (Fig.3). The plates had depressions of different quantities, sizes and types of arrangement (corridor or staggered) on the surface. The material of the plates was aluminum alloy. The length of all plates was 200 mm, the width 100 mm and the thickness 4 mm. The

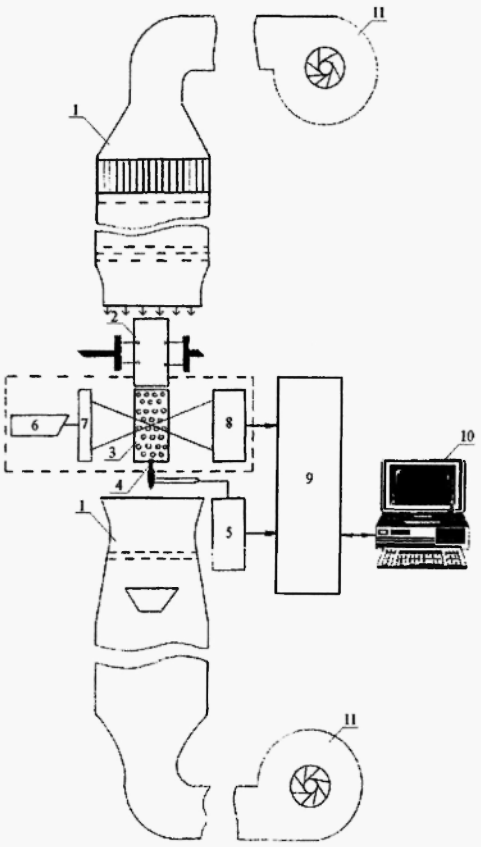

Fig. 2: Aerodynamic bench: 1 – wind-channel 2 – additional plate; 3 – investigating plate; 4 – holder; 5 – three-component strain-measuring device; 6 – laser; 7 – sending optics; 8 – receiving optics; 9 – registering, processing and controlling system; 10 – PC; 11 – blowers.

aerodynamic weight of the plates was measured with the help of a three-component strain-measuring device. Traditionally, aerodynamic weighing uses the method of a loaded element, based on the measuring of drag force, which acts on some surface element, selected from the streamlining body /3/. This method assumes the linear size of the loaded element to be very small (of the order of several millimeters in the downstream direction). It is evident that the loaded element has to model the whole investigated surface or some part of it, i.e., the surface has to be homogeneous. In the given test series the plates had surfaces with hemispherical depressions. The diameter of the depressions was 7-15 mm with a depth of 0.5 mm and 1.6 mm, and the center-to-center spacing of the depressions was 12-19 mm. It was therefore impossible, in principle, to select some small loaded element that would reproduce a whole surface. We have applied a modification of the method of a loaded element. The core of the proposed modification was that we used an additional flat plate with a window in it. The testing plate

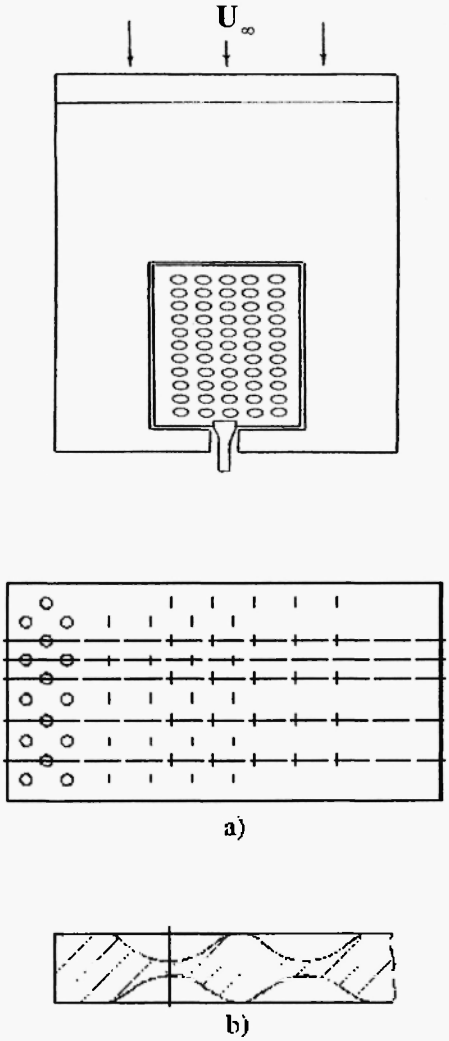

Fig. 3: Schematic of a plate covered with depressions: a) surface view; b) cross-section of plate.

was installed in this window flush with the additional plate. The clearance between the two plates was very small. The additional plate (Fig.3) was rigidly fixed in the working space of the wind-channel, while the testing plate was installed on a three-component strain-measuring device with the help of a special holder .

The aerodynamic weight of the testing plate F_p was determined as follows:

$$F_p=F_{p+h}-F_h \tag{2.1}$$

where F_{p+h} is the total aerodynamic weight of the testing plate and the holder; F_h is the aerodynamic weight of the holder. It should be noted that F_h was measured separately, when the testing plate was installed above the holder, i.e., the holder was in the domain of the plate wake.

Using the obtained F_p, the aerodynamic drag coefficient C_f was calculated:

$$C_f = \frac{F_p g}{\frac{\rho U_\infty^2}{2} S_p}, \tag{2.2}$$

where $g=9.8$ m/s^2 is the free fall acceleration; $S_p=0.0416$ m^2 is the surface area of the testing plate without taking into account the surface of depressions; ρ is the density of the stream flow for the given temperature; U_∞ is the axial velocity of the stream flow. The distribution of the stream velocity component of the flow in the boundary layer near the plate surface was measured with the help of a laser Doppler anemometer (LDA) (pos.6,7,8, Fig.2) /4/ and used for monitoring of flow regimes.

The accuracy of measurement of the aerodynamic weight depended substantially on vibration caused by the blowers and vibration of the plate in the flow. The error of the strain-measuring device due to vibration caused by the blowers was within 1% of the measured weights. The error from vibration of the plate in the flow depended on the stream flow velocity and it was 15% of the average values of the weight for the plate installed on the holder and 5% for holder separately at $U_\infty = 22$ m/s. So, it can be assumed that the total error of measurements of the aerodynamic weight was within 15%. The aerodynamic drag coefficients, measured on both smooth and extended plates, as the final results of the experimental work, are shown in Fig. 4. This figure obviously indicates that there are some shapes of surfaces with hemispherical depressions that do not produce any significant increase in the drag.

3. NUMERICAL CALCULATIONS

Our next concern is preliminary numerical modelling of the flow near the grooves. This modelling starts with a study of the processes inside and around a single depression. In our experiment we could not measure the velocity field inside the depression, because of the resolution of the experiment which did not allow measurements in depressions about 1-2 mm. A thick boundary layer was generated by a special procedure and some results describing the flow near a circular cavity (see Fig.5) were presented in /5/. In these experiments, the ratio of the thickness of the boundary layer to the size of the depression has been approximately equal to the value used in our experiments. Therefore, we have modelled a further experiment /5/. However, for direct modelling even of experiment /5/ we should use a non-orthogonal grid and compute a three-dimensional problem. For preliminary computations we have studied a two-dimensional approximation of this problem and expected to observe, at the starting point,

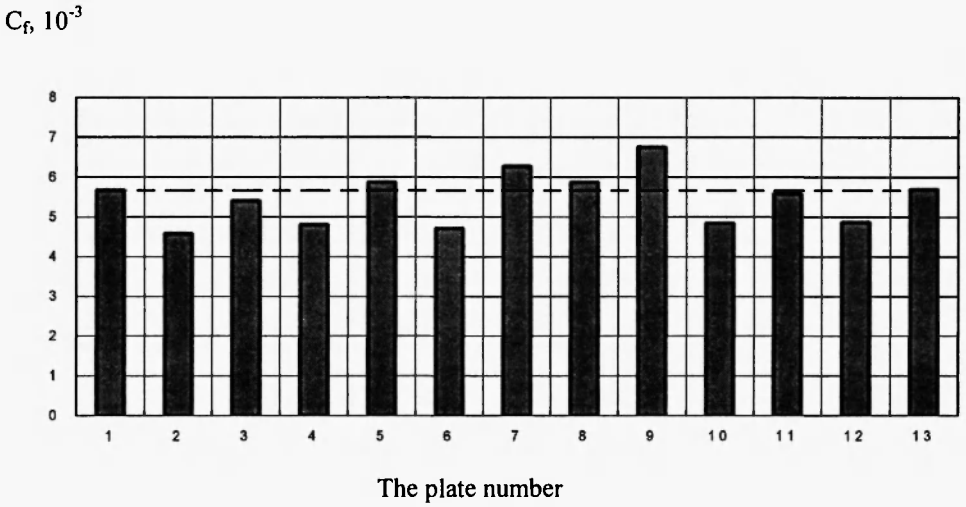

Fig. 4: Aerodynamic drag coefficient C_f for the plates with different sizes of depressions and their locations on the plates for U_∞ = 9.4 m/s (a) and 22 m/s (b), first bar shows C_f for smooth plate.

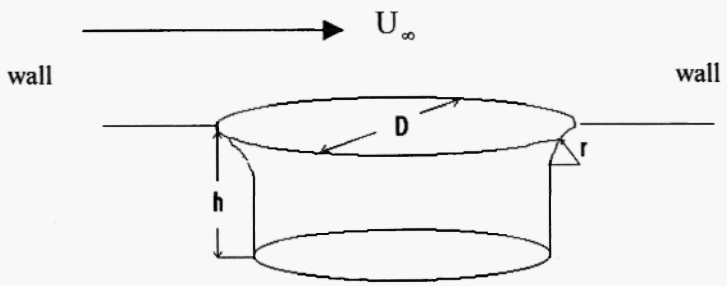

Fig. 5: View of the cavity used in experiment /5/.

the influence of a curvilinear boundary.

The mean flow equations for two-dimensional turbulent flow are used in the standard form (named Reynolds – averaged Navier-Stokes equations (RANS)) /6/:

Mass conservation (continuity equation):

$$\frac{\partial(\rho U)}{\partial x}+\frac{\partial(\rho V)}{\partial y}=0 \tag{3.1}$$

Conservation of x-momentum

$$\frac{\partial(\rho U)}{\partial t}+\frac{\partial}{\partial x}(\rho U^2+\overline{\rho u^2})+\frac{\partial}{\partial y}(\rho UV+\overline{\rho uv})=-\frac{\partial P}{\partial x} \tag{3.2}$$

Conservation of y-momentum

$$\frac{\partial(\rho V)}{\partial t}+\frac{\partial}{\partial x}(\rho UV+\overline{\rho uv})+\frac{\partial}{\partial y}(\rho V^2+\overline{\rho v^2})=-\frac{\partial P}{\partial y} \tag{3.3}$$

In these equations, U and V are the velocities in the x – and y- direction. The symbol t denotes time, and ρ as above is the density of the fluid. P stands for the difference of the static pressure P_s and the hydrostatic pressure. Here all capital letter variables and the fluid properties must be interpreted as time-averaged, as we consider steady flow. Fluctuating quantities are denoted by lower case symbols. Averages are indicated by overbars. The Reynolds stresses $-\overline{\rho u^2}$, $-\overline{\rho uv}$, $-\overline{\rho v^2}$ are related to known quantities via the $\mathbf{k}-\varepsilon$ turbulence model to enable a closed solution of the flow equations. The corresponding equations of the $\mathbf{k}-\varepsilon$ turbulence model according to /7/ are

$$\frac{\partial(\rho k)}{\partial t}-\frac{\partial}{\partial x}(\rho Uk-\frac{\mu_t}{\sigma_k}\frac{\partial k}{\partial x})+\frac{\partial}{\partial y}(\rho Vk-\frac{\mu_t}{\sigma_k}\frac{\partial k}{\partial y})=P_k-\rho\varepsilon, \tag{3.4}$$

$$\frac{\partial(\rho\varepsilon)}{\partial t}-\frac{\partial}{\partial x}(\rho U\varepsilon-\frac{\mu_t}{\sigma_k}\frac{\partial \varepsilon}{\partial x})+\frac{\partial}{\partial y}(\rho V\varepsilon-\frac{\mu_t}{\sigma_k}\frac{\partial \varepsilon}{\partial y})=\frac{\varepsilon}{k}(c_{\varepsilon 1}P_k-c_{\varepsilon 2}\rho\varepsilon), \tag{3.5}$$

$$\mu_t=\rho c_\mu\frac{\mu_t}{\sigma_k}\frac{k^2}{\varepsilon}, \tag{3.6}$$

$$P_k=\mu_t[2(\frac{\partial U}{\partial x})^2+2(\frac{\partial V}{\partial y})^2+(\frac{\partial U}{\partial y}+\frac{\partial V}{\partial x})^2], \tag{3.7}$$

where $c_{\varepsilon 1}, c_{\varepsilon 2}, \sigma_k, \sigma_\varepsilon$ and c_μ are empirical constants, which take on the standard values proposed in /7/.

Our modelling is carried out by calculating a set of equations with the help of the SIMPLE

pressure-velocity coupling algorithm, based on the finite volume discretization scheme extended to a non-orthogonal grid (see /8/). The convective terms are discretized by using a deferred correction scheme. The diffusive terms are generally discretized by applying a central difference scheme. In order to solve the system of equations, a strongly implicit procedure, SIP by Stone /9/ is used, which is based on an incomplete L U – decomposition technique.

In our computations we used data from experiment /5/, namely, identical dimensions and the profiles of the longitudinal component of the mean velocity and turbulence intensity for the inlet boundary conditions. The results comprise distributions of the velocity, pressure and turbulent kinetic energy of the flow near and inside of the grooves. Comparisons between values found experimentally in /5/ and obtained numerically by us for the mean velocity and longitudinal turbulence intensity for h/D=0.2 and for r/R=0 are shown in Figs. 6 and 7. One can see that the agreement between the experimental and numerical results is much better in regions close to the center, where results for the two-dimensional case approach the results of the three-dimensional case. At the same time, the agreement between the experimental and numerical results for longitudinal turbulence intensity is poorer, for many reasons, including accuracy of the experimental data. The sought comparison between distributions of wall-shear stress inside the rectangular and semicircular grooves is shown in Fig.8.

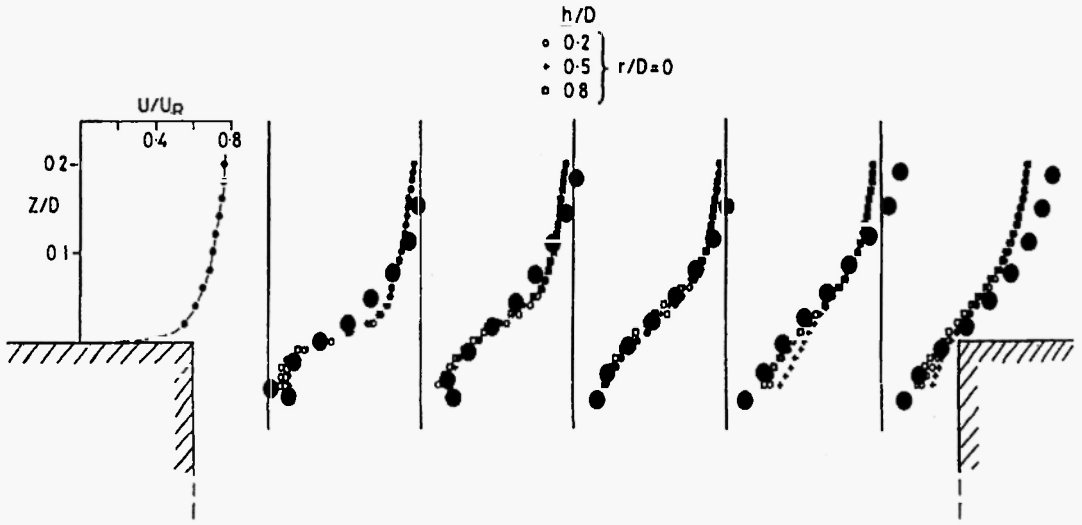

Fig. 6: Vertical profiles of longitudinal mean velocity in the shear layer on the plane of symmetry (Z = 0) for cavity r/D = 0, • – denotes the numerical results for a rectangular groove h/D = 0.2.

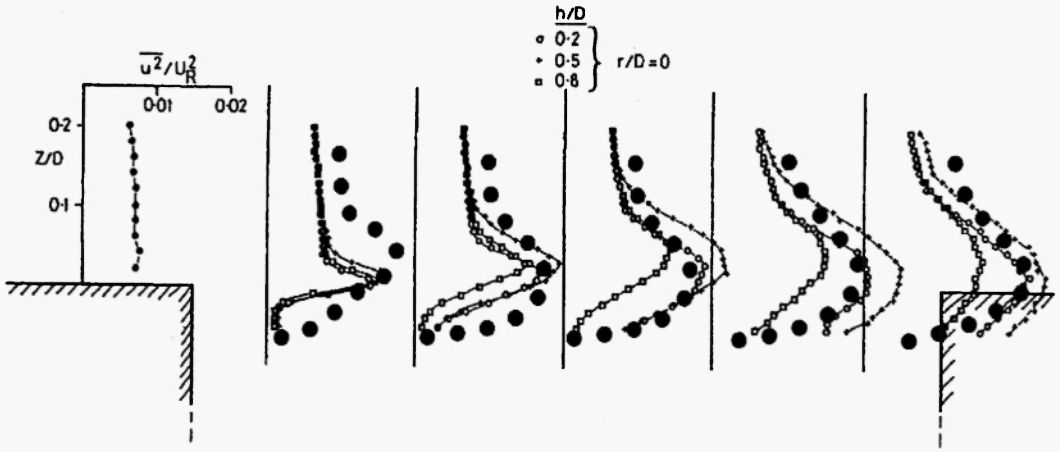

Fig. 7: Vertical profiles of longitudinal turbulence intensity in the shear layer on the plane of symmetry (Z = 0) for cavity r/D = 0, • – denotes the numerical results for a rectangular groove h/D = 0.2.

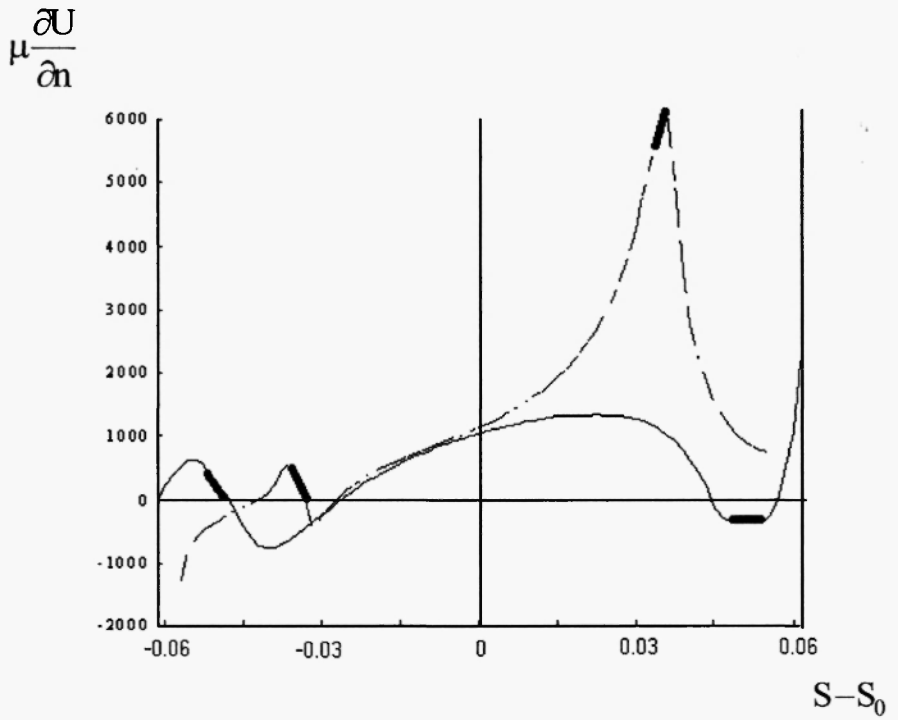

Fig. 8: Distribution of wall-shear stress versus the distance along the groove (dashed line corresponds to semicircular and solid line to rectangular grooves, S_0 – center of the groove, ▬ – boundary regions for different zones of calculations, h/D = 0.015, and ratio r/R for semicircular groove was 0.1).

4. DISCUSSION AND CONCLUDING REMARKS

In /1/ it was experimentally shown that, in the flow near a hemispherical depression regimes accompanied by the effect of drag reduction occur. Our experimental data confirm this effect. A theoretical explanation for this phenomenon was given in /1/, namely, that inside the flow near the hemispherical depression, a stable tornado-like vortex column is formed and this structure stimulates the appearance of the above-mentioned flow regimes. Such a structure was observed with the aid of the visualization method only in one work /1/. However, in experiments with similar grooves, cylindrical cavities with circular edges /5/, the given vortical structure was not indicated. In this work the influence of the depression curvature leads to an increased aerodynamic drag. A similar result is pointed out in our two-dimensional numerical calculations; the curvilinear boundary produces an increase in the tangential velocity in the forward part of the depression as well as an increase in the aerodynamic drag.

With this concern in mind we can offer another explanation for the drag reduction along a surface covered with hemispherical depressions. It is shown /10/ that flow inside a hemispherical depression forms a two-dimensional vortex, whose maximum generates oscillations dependent on the flow parameters and the size of the depression. Also, it is shown that external perturbations in this case can cause the resonant motion of a vortex in a single depression, with shedding of the vortexes in the main flow. This could be a possible reason for convective heat transfer enhancement and drag reduction. The external perturbations produced by the flow distortion from other depressions result in a combined effect of the flow structure generated from the whole extended surface. The drag reduction revealed in our experiments for the special type, size and number of grooves with their arrangement along the surface confirmed this concept.

The complexity of the phenomena observed in our investigation, along with others, supports the need for further research and practical application owing to their technological advantages.

5. ACKNOWLEDGEMENT

This work was supported by the Estonian Scientific Foundation (Grant No. 3493).

REFERENCES

1. G.I. Kiknadze, U.K. Krasnov, N.F. Podimako and V.B. Habenski, *Dokl. Akad. Nauk SSSR*, **291**, No 6, 1986; p.1315. (in Russian).
2. U.M. Mshvidobadze and I. 1. Mitrohin, in: *Modern Problem of Thermophysics*, Novosibirsk, 1988; p.33 (in Russian).

3. I.L. Povh, in: *Aerodynamic Experiment in Machine Building*. Inostrannaja Literatura, Moscow, 1974 (in Russian).
4. M. Hussainov, A. Kartushinsky, Ü. Rudi and S. Tisler, *Int. J. Multiphase Flow*, **21**, 1995, p.1141.
5. E.Savory, E., Toy, N., and Gaudet, L.,in: *Emerging Techniques in Drag Reduction*, The Ipswich Book Company, Suffolk, UK, 1996, p.317.
6. T. Cebeci and A.M.O. Smith, *Analysis of Turbulent Boundary Layers*, Academic Press, New York, 1974.
7. B.E. Launder and D.B. Spalding, *Comp. Meth. Appl. Mech. Eng.*, **3**, 1974, p. 269.
8. Joel H. Ferziger and M. Peric, *Computational Methods for Fluid Dynamics*, Springer-Verlag, Berlin, Heidelberg, New York, 1996.
9. H.L. Stone, *SIAM J. Numer. Anal.*, **5**, 1968, p.530.
10. V. Gorban and I. Gorban, AGARD REPORT 827, High Speed Body Motion in Water, France, 1998, p.15-1.